

ORIGINAL ARTICLE

SDSS 2022
The International Colloquium on Stability
and Ductility of Steel Structures
14-16 September, University of Aveiro, Portugal

Dimensioning Aids for Stiffened and Unstiffened Plates According to Eurocode 3 Part 1-5

Felix Hulm¹, Johannes Kreutz¹, Nadine Maier², Martin Mensinger², Joseph Ndogmo²

Correspondence

Dr. Joseph Ndogmo
Technical University Munich
Chair of Metal Structures
Arcisstraße 21
80333 Munich
Email: ndogmo@bv.tum.de

Abstract

In Germany stiffened plate in bridge construction must be verified using the method of reduced stresses (MRS) according to DIN EN 1993-1-5 [2, 3]. Unstiffened plates on the other hand may be verified either according to the effective widths method or according to the reduced stress method. In order to shorten the time-consuming verification of the standardised verification formats for pre-dimensioning which is particularly prevalent for stiffened plates diagrams are developed and presented in the present paper on the basis of the MRS by reformulating the buckling verification which enable a quick pre-dimensioning. With the diagrams, the dimensioning of plate thicknesses and stiffener spacings can be carried out in a few simple and comprehensible steps. The diagrams are selected on the basis of the geometry parameters a , b , and t or the applicable boundary conditions. For stiffened plate, the maximum permissible spacing of the longitudinal stiffeners or the required main plate thickness can be determined. Diagrams for the dimensioning of longitudinal stiffeners by determining minimum stiffnesses are also presented. The minimum stiffnesses are derived from the geometry of the linear buckling shapes of simply stiffened plate.

Keywords

Plate buckling; buckling panel; minimum stiffness; longitudinal stiffeners

1 Introduction

The design according to the method of reduced stresses (MRS) according to DIN EN 1993-1-5 (see [2, 3]) has been introduced and established by the building authorities in Germany as the only design method for the design of stiffened plate in bridge construction. For the common situations with rectangular buckling panels with Navier support of all edges and stress distribution, the critical load amplifier can be determined directly with approximation formulas. For general geometries and stress ratios but especially for stiffened plates a numerical determination of the critical load amplifier, e.g. with the help of finite element models, is often an unavoidable intermediate step within the verification. The diagrams for the verification of the unstiffened panels are based on a grouping of the stress states and the conversion of the formulas for the determination of the critical load amplifier and the formulas of the MRS according to DIN EN 1993-1-5. With the present results from this paper, unstiffened plates can be designed with the help of the diagrams shown. The diagrams clearly show the effects of various parameters such as slenderness or stress distribution. The engineer can thus adjust the necessary parameters in the design phase in order to reach the goal of an adequate preliminary design quickly and efficiently.

The dimensioning of longitudinally stiffened plates presented in this paper is carried out in a two-step procedure. In a first step, the stiffener spacing or the plate thicknesses are determined with the help of the dimensioning aids for unstiffened plates in such a way that subpanel buckling is excluded. For the dimensioning of the stiffeners, i.e. their dimensions or bending stiffness, diagrams will afterwards also be created. They are based on the systematic numerical linear buckling value analysis of longitudinally stiffened plates. The evaluation of the results is carried out for different geometry, stiffness and stress ratios with the aim of determining the bending stiffness of the longitudinal stiffener in such a way that the subpanel buckling just becomes decisive for stiffened plates. The numerical investigations are carried out using Python routines [4] and the finite element program package SOFiSTiK [5]. The total buckling of the plate is not initially considered in the pre-dimensioning presented and must be equal the column-like behaviour recorded in the course of the subsequent verification.

1.1 Current status of standardisation

Basically, according to DIN EN 1993-1-5 [2] and the associated national annex [3], two verification methods against plate buckling are given. One is the method of effective widths (MWB) and the other is the method of reduced stresses (MRS). The method of

This is an open access article under the terms of the Creative Commons Attribution-NonCommercial-NoDerivs License, which permits use and distribution in any medium, provided the original work is properly cited, the use is non-commercial and no modifications or adaptations are made.

Open Access funding enabled and organized by Projekt DEAL.

WOA Institution: Technische Universität München

Consortia Name: Projekt DEAL

© 2022 The Authors. Published by Ernst & Sohn GmbH. · ce/papers 5 (2022), No. 4

<https://doi.org/10.1002/cepa.1801>

wileyonlinelibrary.com/journal/cepa | 635

reduced stresses is currently the common verification format in Germany for longitudinally stiffened buckling panels in bridge construction. The reduction factors $\rho_{c,x}$, $\rho_{c,z}$ and χ_w of the buckling verification of the whole buckling panel, whose stress state is defined by the components $\sigma_{x,Ed}$, $\sigma_{z,Ed}$ and τ_{Ed} and the stress ratio Ψ (see figure 1), are calculated on the basis of a global system slenderness $\bar{\lambda}_p$ calculated. In contrast to the MRS, the applicability is not restricted by standards and, with the help of an FE-supported verification, non-uniform buckling panels or plates with larger recesses can also be verified. The formulas of the verification according to the MRS can be taken from DIN EN 1993-1-5 [2, 3].

2 Excluding the buckling of the sub-panel with the help of diagrams

For an alternative representation of the buckling verification with the help of diagrams, the formulas of DIN EN 1993-1-5 [2, 3] are reformulated. By means of a few simplifications, in particular the introduction of a proportional shear stress ($\beta_\tau \cdot \sigma_{x,Ed}$) or transverse compressive stress ($\beta \cdot \sigma_{x,Ed}$) instead of the absolute stress values, the formulas can be converted according to the reduced stress method and resolved to σ_x . By determining the stresses that can be absorbed for a previously defined buckling panel geometry, it enables the evaluation of the verification concept in the form of diagrams. The parameters that flow into the formulas are shown in Figure 1.

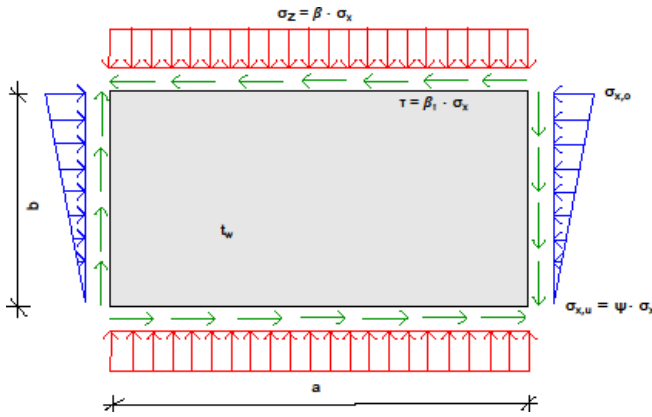


Figure 1 Unstiffened buckling panel with the introduced parameters β_τ and β

2.1 Restrictions

For buckling panels without stiffeners, the verification according to the MRS in accordance with DIN-EN-1993-1-5 [2, 3] is possible without a preceding computer-aided calculation to determine the critical load increase factors. This means that the purely formula-based buckling verification for unstiffened plates can be converted and resolved to σ_x . For longitudinally stiffened plates, the presented procedure is only applicable to exclude local buckling. It cannot replace the global buckling verification of the whole plate. To this purpose, minimum stiffnesses of the longitudinal stiffeners to prevent global buckling are presented in the following part 3 of this paper.

For the determination of the stresses that can be supported for a given buckling panel geometry, the following assumptions and limitations are made:

- At all edges the buckling panel is non-displaceable and hinge supported (Navier's boundary conditions).
- Restriction of a diagram to a fixed boundary stress ratio ψ .
- The diagrams depend on the steel grade.

- Shear stresses are taken into account in the following calculations and diagrams via a shear component $\beta_\tau = \tau_{Ed} / \sigma_{x,Ed}$.
- Transverse compressive stresses are taken into account in the following calculations and diagrams via a transverse pressure component $\beta = \sigma_{z,Ed} / \sigma_{x,Ed}$.
- The maximum transverse compressive stress is applied over the entire length of the buckling panel on both sides (conservative assumption).
- Local initiation of compressive stresses is not covered by the diagrams so far.
- Shear stresses and transverse compression are not considered simultaneously.
- The geometry is described by a buckling panel slenderness.

The procedure for creating diagrams explained below can be extended to most common use cases.

2.2 Reformulation of the formulae of the reduced stress method

In the following, the global system slenderness $\bar{\lambda}_p$ depending on the total stress ratio is derived. This is the basis for the creation of the diagrams. The procedure is shown on the one hand for combined longitudinal and shear stress and on the other hand for biaxial stress states consisting of longitudinal and transverse compressive stresses. The formulas for the determination of the reduction factors $\rho_{c,x}$, $\rho_{c,z}$ and χ_w can be taken from DIN EN 1993-1-5 [2,3]. The column-like behaviour is taken into account here. A repetition of this phenomenon will be omitted here.

2.2.1 Longitudinal and shear stresses

The formulas for developing the diagrams for unstiffened plate under combined longitudinal and shear stresses are explained below.

$$\sigma_E = \frac{\pi^2 \cdot E}{12 \cdot (1 - \nu^2)} \cdot \left(\frac{t}{b}\right)^2 \quad (1)$$

$$\sigma_{cr,x} = k_\sigma \cdot \sigma_E \quad (2)$$

$$\tau_{cr} = k_\tau \cdot \sigma_E \quad (3)$$

$\alpha_{ult,k}$ is the smallest magnification factor of the design loads to achieve the equivalent stress σ_v of the panel according to Von-Mises. By introducing a shear component $\beta_\tau = \tau_{Ed} / \sigma_{x,Ed}$ it is possible to isolate $\sigma_{x,Ed}$ and extract it from the root.

$$\begin{aligned} \alpha_{ult,k} = \frac{f_y}{\sigma_v} &= \frac{f_y}{\sqrt{\sigma_{x,Ed}^2 + 3 \cdot \tau_{Ed}^2}} = \frac{f_y}{\sqrt{\sigma_{x,Ed}^2 + 3 \cdot (\beta_\tau \cdot \sigma_{x,Ed})^2}} \\ &= \frac{f_y}{\sigma_{x,Ed} \cdot \sqrt{1 + 3 \cdot \beta_\tau^2}} \end{aligned} \quad (4)$$

In addition, an isolation of $\sigma_{x,Ed}$ may occur in the formula for the critical load increase factor α_{cr} , using the shear component β_τ .

$$\alpha_{cr,x} = \frac{\sigma_{cr,x}}{\sigma_{x,Ed}} \quad (5)$$

$$\alpha_{cr,\tau} = \frac{\tau_{cr}}{\tau_{Ed}} \quad (6)$$

$$\begin{aligned}
\frac{1}{\alpha_{cr}} &= \frac{1+\psi}{4 \cdot \alpha_{cr,x}} + \sqrt{\left(\frac{1+\psi}{4 \cdot \alpha_{cr,x}}\right)^2 + \frac{1-\psi}{2 \cdot \alpha_{cr,x}^2} + \frac{1}{\alpha_{cr,\tau}^2}} \\
&= \frac{1+\psi}{4 \cdot \alpha_{cr,x}} + \sqrt{\frac{(1+\psi)^2}{16 \cdot \alpha_{cr,x}^2} + \frac{1-\psi}{2 \cdot \alpha_{cr,x}^2} + \frac{1}{\alpha_{cr,\tau}^2}} \\
&= \frac{(1+\psi) \sigma_{x,Ed}}{4 \cdot \sigma_{cr,x}} + \sqrt{\frac{(1+\psi)^2 \cdot \sigma_{x,Ed}^2}{16 \cdot \sigma_{cr,x}^2} + \frac{(1-\psi) \cdot \sigma_{x,Ed}^2}{2 \cdot \sigma_{cr,x}^2} + \frac{\sigma_{x,Ed}^2 \cdot \beta_\tau^2}{\tau_{cr}^2}} \\
&= \frac{(1+\psi) \cdot \sigma_{x,Ed}}{4 \cdot \sigma_{cr,x}} + \sigma_{x,Ed} \cdot \sqrt{\frac{(1+\psi)^2}{16 \cdot \sigma_{cr,x}^2} + \frac{1-\psi}{2 \cdot \sigma_{cr,x}^2} + \frac{\beta_\tau^2}{\tau_{cr}^2}}
\end{aligned} \tag{7}$$

$$\begin{aligned}
\alpha_{cr} &= \frac{1}{\frac{(1+\psi) \cdot \sigma_{x,Ed} + \sigma_{x,Ed}}{4 \cdot \sigma_{cr,x}} + \sigma_{x,Ed} \cdot \sqrt{\frac{(1+\psi)^2}{16 \cdot \sigma_{cr,x}^2} + \frac{1-\psi}{2 \cdot \sigma_{cr,x}^2} + \frac{\beta_\tau^2}{\tau_{cr}^2}}} = \\
&= \frac{1}{\sigma_{x,Ed} \left(\frac{1+\psi}{4 \cdot \sigma_{cr,x}} + \sqrt{\frac{(1+\psi)^2}{16 \cdot \sigma_{cr,x}^2} + \frac{1-\psi}{2 \cdot \sigma_{cr,x}^2} + \frac{\beta_\tau^2}{\tau_{cr}^2}} \right)}
\end{aligned} \tag{8}$$

This shortens $\sigma_{x,Ed}$ from the formula for the global system slenderness $\bar{\lambda}_p$, whereby this can be determined independently of the magnitude of the stresses.

$$\begin{aligned}
\bar{\lambda}_p &= \sqrt{\frac{\alpha_{ult,k}}{\alpha_{cr}}} = \sqrt{\frac{\frac{f_y}{\sigma_{x,Ed} \cdot \sqrt{1+\beta^2}}}{\frac{1}{\sigma_{x,Ed} \left(\frac{1+\psi}{4 \cdot \sigma_{cr,x}} + \sqrt{\frac{(1+\psi)^2}{16 \cdot \sigma_{cr,x}^2} + \frac{1-\psi}{2 \cdot \sigma_{cr,x}^2} + \frac{\beta_\tau^2}{\tau_{cr}^2}} \right)}}}} = \\
&= \sqrt{\frac{f_y}{\sqrt{1+\beta^2}} \cdot \left(\frac{1+\psi}{4 \cdot \sigma_{cr,x}} + \sqrt{\frac{(1+\psi)^2}{16 \cdot \sigma_{cr,x}^2} + \frac{1-\psi}{2 \cdot \sigma_{cr,x}^2} + \frac{\beta_\tau^2}{\tau_{cr}^2}} \right)}
\end{aligned} \tag{9}$$

The further reduction factors including those from column-like behaviour are exclusively dependent on the global system slenderness and the geometry when using the reduced stress method and can therefore be determined. The basis for the evaluation diagrams is the verification formula 10.5 of DIN EN 1993-1-5 [2]. It should be noted that this formula does not represent a linear utilisation factor but merely contains a statement about the fulfilment or non-fulfilment of the buckling verification. To obtain a linear utilisation factor η , by taking the square root of the term analogous to the Von-Mises equivalent stress is a target-oriented solution. Finally, after setting the utilisation factor η to 1.0 and using the above-mentioned substitutions the equation can be solved and lead to $\sigma_{x,Ed}$.

$$\left(\frac{\sigma_{x,Ed}}{\rho_{c,x} f_y / \gamma_{M1}} \right)^2 + 3 \cdot \left(\frac{\tau_{Ed}}{\chi_w f_y / \gamma_{M1}} \right)^2 = 1,0 \tag{10}$$

$$\left(\frac{\sigma_{x,Ed}}{\rho_{c,x} f_y / \gamma_{M1}} \right)^2 + 3 \cdot \left(\frac{\beta_\tau \sigma_{x,Ed}}{\chi_w f_y / \gamma_{M1}} \right)^2 = 1,0 \tag{11}$$

$$\max \sigma_{x,Ed} = \frac{1}{\sqrt{\left(\frac{1}{\rho_{c,x} f_y / 1,1} \right)^2 + 3 \cdot \left(\frac{\beta_\tau}{\chi_w f_y / 1,1} \right)^2}} \tag{12}$$

This represents the maximum longitudinal stress which can be applied by the specified buckling panel together with a proportion of the shear stress $\tau_{Ed} = \beta_\tau \cdot \sigma_{x,Ed}$ while using the method of reduced stresses (MRS).

2.2.2 Longitudinal and transverse compressive stresses

$$\sigma_{E,x} = \frac{\pi^2 \cdot E}{12 \cdot (1-\nu^2)} \cdot \left(\frac{t}{b} \right)^2 \tag{13}$$

$$\sigma_{E,z} = \frac{\pi^2 \cdot E}{12 \cdot (1-\nu^2)} \cdot \left(\frac{t}{a} \right)^2 \tag{14}$$

$$\sigma_{cr,x} = k_{\sigma,x} \cdot \sigma_{E,x} \tag{15}$$

$$\sigma_{cr,z} = k_{\sigma,z} \cdot \sigma_{E,z} \tag{16}$$

To calculate the critical stress, it is necessary to determine the buckling value $k_{\sigma,z}$, which depends on α . Since $1/\alpha$ for the subpanel under transverse compression is usually less than 1,0, $k_{\sigma,z}$ is determined in the context of this paper via the following formula.

$$k_{\sigma,z} = (1/\alpha + \alpha)^2 \tag{17}$$

By introducing the transverse compression component $\beta = \sigma_{z,Ed} / \sigma_{x,Ed}$ it is also possible to isolate $\sigma_{x,Ed}$ for biaxial stress conditions in the following formulae.

$$\begin{aligned}
\alpha_{ult,k} &= \frac{f_y}{\sigma_v} = \frac{f_y}{\sqrt{\sigma_{x,Ed}^2 + \sigma_{z,Ed}^2 - \sigma_{x,Ed} \sigma_{z,Ed}}} = \frac{f_y}{\sqrt{\sigma_{x,Ed}^2 + (\beta \cdot \sigma_{x,Ed})^2 - \sigma_{x,Ed} \cdot \beta \cdot \sigma_{x,Ed}}} = \\
&= \frac{f_y}{\sigma_{x,Ed} \cdot \sqrt{1 + \beta^2 - \beta}}
\end{aligned} \tag{18}$$

$$\alpha_{cr,x} = \frac{\sigma_{cr,x}}{\sigma_{x,Ed}} \tag{19}$$

$$\alpha_{cr,z} = \frac{\sigma_{cr,z}}{\sigma_{z,Ed}} \tag{20}$$

$$\begin{aligned}
\frac{1}{\alpha_{cr}} &= \frac{1}{\alpha_{cr,x}} + \frac{1}{\alpha_{cr,z}} + \sqrt{\left(\frac{1+\psi}{4 \cdot \alpha_{cr,x}} + \frac{1+1}{4 \cdot \alpha_{cr,z}} \right)^2 + \frac{1-\psi}{2 \cdot \alpha_{cr,x}^2} + \frac{1-1}{2 \cdot \alpha_{cr,z}^2}} \\
&= \frac{1+\psi}{4 \cdot \alpha_{cr,x}} + \frac{1}{2 \cdot \alpha_{cr,z}} \\
&+ \sqrt{\frac{(1+\psi)^2}{16 \cdot \alpha_{cr,x}^2} + \frac{1}{4 \cdot \alpha_{cr,z}^2} + \frac{2(1+\psi) \cdot 2}{16 \cdot \alpha_{cr,x} \alpha_{cr,z}} + \frac{1-\psi}{2 \cdot \alpha_{cr,x}^2}} \\
&= \frac{(1+\psi) \sigma_{x,Ed}}{4 \cdot \sigma_{cr,x}} + \frac{\beta \cdot \sigma_{x,Ed}}{2 \cdot \sigma_{cr,z}} + \sigma_{x,Ed} \\
&\cdot \sqrt{\frac{(1+\psi)^2}{16 \cdot \sigma_{cr,x}^2} + \frac{\beta^2}{4 \cdot \sigma_{cr,z}^2} + \frac{(1+\psi) \cdot \beta}{4 \cdot \sigma_{cr,x} \sigma_{cr,z}} + \frac{1-\psi}{2 \cdot \sigma_{cr,x}^2}}
\end{aligned} \tag{21}$$

$$\begin{aligned}
\alpha_{cr} &= \frac{1}{\frac{(1+\psi) \sigma_{x,Ed}}{4 \cdot \sigma_{cr,x}} + \frac{\beta \cdot \sigma_{x,Ed}}{2 \cdot \sigma_{cr,z}} + \sigma_{x,Ed} \cdot \sqrt{\frac{(1+\psi)^2}{16 \cdot \sigma_{cr,x}^2} + \frac{\beta^2}{4 \cdot \sigma_{cr,z}^2} + \frac{(1+\psi) \cdot \beta}{4 \cdot \sigma_{cr,x} \sigma_{cr,z}} + \frac{1-\psi}{2 \cdot \sigma_{cr,x}^2}}} = \\
&= \frac{1}{\sigma_{x,Ed} \cdot \left(\frac{1+\psi}{4 \cdot \sigma_{cr,x}} + \frac{\beta}{2 \cdot \sigma_{cr,z}} + \sqrt{\frac{(1+\psi)^2}{16 \cdot \sigma_{cr,x}^2} + \frac{\beta^2}{4 \cdot \sigma_{cr,z}^2} + \frac{(1+\psi) \cdot \beta}{4 \cdot \sigma_{cr,x} \sigma_{cr,z}} + \frac{1-\psi}{2 \cdot \sigma_{cr,x}^2}} \right)}
\end{aligned} \tag{22}$$

$$\begin{aligned}
\bar{\lambda}_p &= \sqrt{\frac{\alpha_{ult,k}}{\alpha_{cr}}} = \sqrt{\frac{\frac{f_y}{\sigma_{x,Ed} \cdot \sqrt{1+\beta^2-\beta}}}{\frac{1}{\sigma_{x,Ed} \cdot \left(\frac{1+\psi}{4 \cdot \sigma_{cr,x}} + \frac{\beta}{2 \cdot \sigma_{cr,z}} + \sqrt{\frac{(1+\psi)^2}{16 \cdot \sigma_{cr,x}^2} + \frac{\beta^2}{4 \cdot \sigma_{cr,z}^2} + \frac{(1+\psi) \cdot \beta}{4 \cdot \sigma_{cr,x} \sigma_{cr,z}} + \frac{1-\psi}{2 \cdot \sigma_{cr,x}^2}} \right)}}}} = \\
&= \sqrt{\frac{f_y}{\sqrt{1+\beta^2-\beta}} \cdot \left(\frac{1+\psi}{4 \cdot \sigma_{cr,x}} + \frac{\beta}{2 \cdot \sigma_{cr,z}} + \sqrt{\frac{(1+\psi)^2}{16 \cdot \sigma_{cr,x}^2} + \frac{\beta^2}{4 \cdot \sigma_{cr,z}^2} + \frac{(1+\psi) \cdot \beta}{4 \cdot \sigma_{cr,x} \sigma_{cr,z}} + \frac{1-\psi}{2 \cdot \sigma_{cr,x}^2}} \right)}
\end{aligned}$$

(23)

The other reduction factors are exclusively dependent on the global slenderness $\bar{\lambda}_p$ and the geometry and can therefore be determined. The degree of utilisation is set to $\eta = 1,0$. As in section 2.2.1 for buckling panels with longitudinal and shear stresses, a linear utilisation factor is also determined here analogous to the Von-Mises equivalent stress. The result is an absorbable longitudinal and transverse compressive stress for the given buckling panel configuration.

$$\left(\frac{\sigma_{x,Ed}}{\rho_{c,x} \cdot f_y / \gamma_{M1}}\right)^2 + \left(\frac{\sigma_{z,Ed}}{\rho_{c,z} \cdot f_y / \gamma_{M1}}\right)^2 - V \cdot \left(\frac{\sigma_{x,Ed}}{\rho_{c,x} \cdot f_y / \gamma_{M1}}\right) \left(\frac{\sigma_{z,Ed}}{\rho_{c,z} \cdot f_y / \gamma_{M1}}\right) = 1,0 \quad (24)$$

$$\left(\frac{\sigma_{x,Ed}}{\rho_{c,x} \cdot f_y / \gamma_{M1}}\right)^2 + \left(\frac{\beta \cdot \sigma_{x,Ed}}{\rho_{c,z} \cdot f_y / \gamma_{M1}}\right)^2 - V \cdot \left(\frac{\sigma_{x,Ed}}{\rho_{c,x} \cdot f_y / \gamma_{M1}}\right) \left(\frac{\beta \cdot \sigma_{x,Ed}}{\rho_{c,z} \cdot f_y / \gamma_{M1}}\right) = 1,0 \quad (25)$$

$$\max \sigma_{x,Ed} = \frac{1}{\sqrt{\left(\frac{1}{\rho_{c,x} \cdot f_y / \gamma_{M1}}\right)^2 + \left(\frac{\beta}{\rho_{c,z} \cdot f_y / \gamma_{M1}}\right)^2 - V \cdot \left(\frac{1}{\rho_{c,x} \cdot f_y / \gamma_{M1}}\right) \left(\frac{\beta}{\rho_{c,z} \cdot f_y / \gamma_{M1}}\right)}} \quad (26)$$

Due to the load introduction over the entire panel length and the use of a buckling value for transverse compression on both sides, the diagrams produced are very much on the safe side, provided that the amount of the maximum acting locally limited transverse compressive stress is applied unabated. Only buckling due to local load application must be investigated separately in the case of very short load application lengths. In the future, the presented procedure can be used, for example, to create additional diagrams with buckling values for a one-sided load with a shorter load introduction length.

2.3 Example of created diagrams

Within the scope of this paper, diagrams are printed as examples for the steel grades S235 and S355, in each case for the boundary stress ratios $\psi = 1,0$ (pure longitudinal compression), $\psi = 0$ (longitudinal compression with bending component) and $\psi = -1$ (pure bending). The generation was carried out using Python scripts [4]. In the diagrams for the longitudinal and shear stresses, only the worst case of an infinitely long plate is considered in the context of the paper. It has been shown that the deviations of the infinitely long plate compared to a plate with equal side lengths ($\alpha = 1,0$) are less than 10%. It is clear from the diagrams in Figure 2 that the absorbable longitudinal stresses and their associated proportional shear stresses increase significantly with increasing transition from constant longitudinal compression to pure bending. With increasing proportional shear stress and thus greater total loading of the panel, the absorbable longitudinal stresses become smaller and smaller. With greater slenderness b/t of the plate, the stresses that can be absorbed also become smaller, as is to be expected. For the dimensioning of panels, for example, a stress state with a given plate height b can be determined in a global structural analysis with freely selected plate thicknesses. On the basis of the existing edge stress ratio ψ and the stress ratio $\beta_\tau = \tau_{Ed} / \sigma_{x,Ed}$ a suitable diagram can be selected. The maximum permissible slenderness b/t can be determined from the diagram. If the plate thickness used in the global structure calculation is too small, the plate thicknesses and stress can be scaled according to the ratio t_{nach} / t_{vor} . In this way, sheet thicknesses or stiffener spacings can be selected very purposefully and efficiently.

While the slenderness b/t of the plate is mainly decisive for the buckling verification due to the longitudinal stresses, the column-like behaviour as a result of the transverse compression is dominated by the aspect ratio a/b . In order to take this effect into account, design diagrams for different aspect ratios α were

developed. The diagrams of the load-bearing behaviour under the influence of transverse compression shown below were drawn up for the aspect ratios $\alpha = 1,0$ (Figure 3/ 4 top), for $\alpha = 2,0$ (Figure 3/ 4 centre) and for $\alpha = 5,0$ (Figure 3/ 4 bottom). It can be seen that buckling panels under transverse compression load can absorb significantly lower stresses with increasing buckling panel length. While the red reference line (without transverse compression) remains the same, the remaining lines of the diagrams decrease significantly with increasing relative buckling panel length.

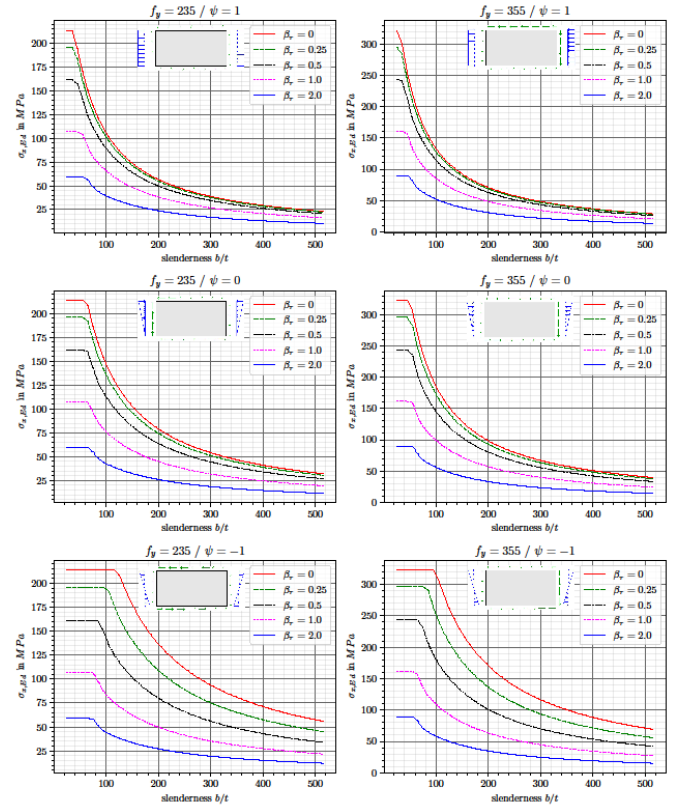


Figure 2 Diagrams for dimensioning unstiffened buckling panels as a function of the edge stress ratio ψ , the proportional shear stress β_τ and the yield strength f_y

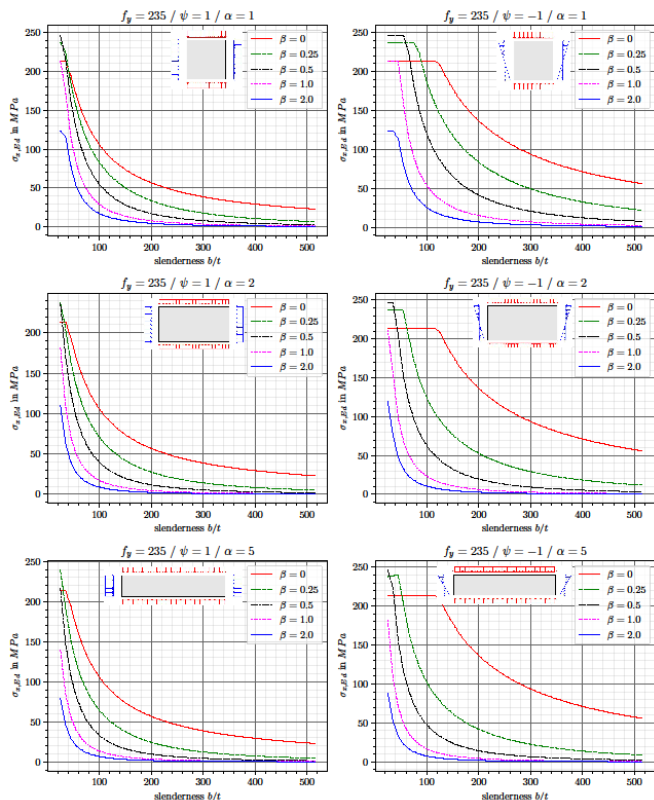


Figure 3 Diagrams for the dimensioning of unstiffened buckling fields as a function of the proportional transverse compressive stress β for a yield strength of the material $f_y = 235 \text{ N/mm}^2$

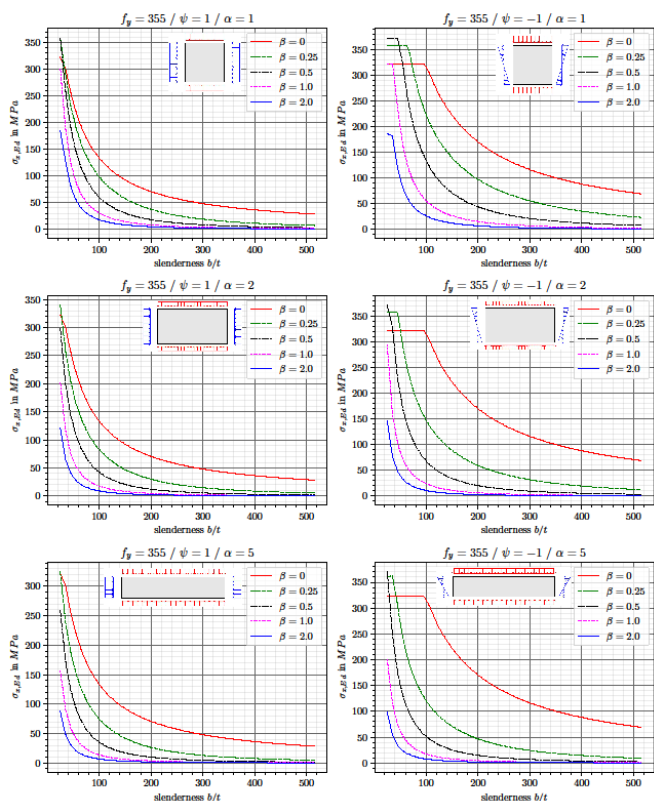


Figure 4 Diagrams for the dimensioning of unstiffened buckling fields as a function of the proportional transverse compressive stress β for a yield strength of the material $f_y = 355 \text{ N/mm}^2$

3 Dimensioning of longitudinal stiffeners based on minimum

stiffnesses

The aim of the present paper is to allow a pre-dimensioning of longitudinal stiffeners in the design phase based on minimum stiffnesses for the longitudinal stiffeners. In the context of this paper, the minimum stiffness is defined as the required area moment of inertia, which leads to the smaller deformation of the stiffener in relation to the deformations of the surrounding subpanels in the linear buckling analysis.

3.1 Numerical determination of the diagram data

The calculation is carried out on a finite element system whereby the buckling panel is modelled with shell elements and the buckling stiffener with beam elements. The beam elements are meshed with the shell elements. For the stiffness, a bar cross-section is defined, the dimensions of which are scaled and thus the stiffness is varied. For the creation of the diagrams shown below, the angular stiffener shown in Figure 5 was used as an example. The participating sheet metal components $b_{i,inf}$ and $b_{i,sup}$ are used for the calculation of the area moment of inertia $I_{sl,1}$ according to DIN EN 1993-1-5 Annex A [3].

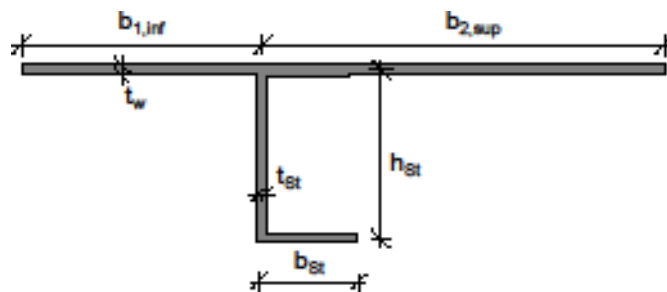


Figure 5 Linear scalable initial stiffener for FEM analyses of buckling panels for the determination of minimum stiffness

$$\gamma = \frac{I_{sl,1}}{I_p} = \frac{I_{sl,1} \cdot 10,92}{b \cdot t^3} \tag{27}$$

The load boundary conditions are now applied to this FEM system and a linear buckling value analysis is performed. The elastic critical buckling mode of this analysis represents the buckling shapes for the applied stress condition. In these displacement fields, the averaged node displacement perpendicular to the plane of all nodes in the system is then related to the averaged displacement of the stiffener nodes. A limit value for this ratio is used to determine the stiffness of the longitudinal stiffener above which it is considered non-displaceable and thus subpanel buckling prevails. A deformation ratio k_u around the value 2.0 has proven to be useful. The diagrams shown in the following were determined with the criterion $k_u = 1.8$. The investigations were carried out for different slendernesses b/t of the main plate and stiffness ratios $\gamma = I_{sl,1}/I_p$. For each slenderness b/t the stiffness of the stiffener is iteratively increased until the longitudinal stiffener in the buckling shape is considered to be non-displaceable according to the defined criterion (cf. formula (28) below). The minimum stiffnesses determined in this way are then presented in the form of diagrams.

$$k_u = \frac{u_{z,average,Stiffener}}{u_{z,average,all}} < 1,8 \tag{28}$$

With

$$u_{z,average,Stiffener} = \frac{\sum_{nodes,Stiffener} u_z}{n_{(nodes,Stiffener)}} \tag{29}$$

$$u_{z,average,all} = \frac{\sum_{nodes} u_z}{n_{(nodes)}} \tag{30}$$

The boundary lines for this criterion are shown in the diagrams (Figures 10 to 12) for different stress and geometry boundary conditions.

3.2 Panels with a central longitudinal stiffener and constant longitudinal compression

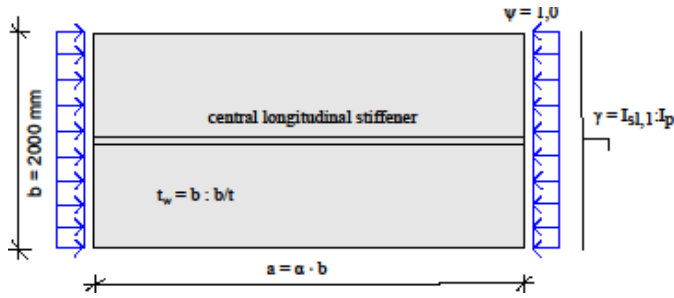


Figure 6 Parameterised buckling panel for the investigation of minimum stiffnesses for a central longitudinal stiffener and constant longitudinal compression

Minimum stiffnesses are determined, among others, for the parameterised buckling panel with a central longitudinal stiffener and constant longitudinal compression shown in Figure 6. Three different aspect ratios are investigated. $\alpha = a/b = 1,0; 2,0; 5,0$. Since the specified buckling panel configuration with constant longitudinal compression represents the worst case, conservative stiffener dimensions can be derived from this consideration. The parameter α influences the buckling length of the stiffener. For longer buckling panels with a larger α a higher minimum stiffness is therefore required to prevent global buckling. The related stiffener slenderness for very slender buckling panels from $b/t > 200$ without transverse compression when considering the investigated buckling panel parameters for long buckling panels $\alpha = 5,0$ and $\psi = 1,0$ and in the range of approx. $\gamma = 30$ (see Figure 12). For thicker-walled plates with a smaller slenderness b/t the minimum stiffnesses required to force local buckling shapes become proportionally larger due to the thicker main plates.

In the national annex of DIN EN 1993-1-5 [3], a minimum stiffness for longitudinal stiffeners is specified for the calculation according to the effective width method. "Longitudinal stiffeners with stiffener cross-sections whose stiffness is $\gamma < 25$ (γ according to DIN EN 1993-1-5:2010-12, Annex A), shall be neglected." [NCI to 4.5.1(3)][3] The reduced stress method is in principle not affected by the minimum stiffness, as the stresses that can be absorbed are reduced across the board. In terms of economy, however, it seems advantageous to dimension stiffeners at least according to the minimum stiffness described above, since the welding effort is not significantly increased by choosing larger stiffeners. Figure 7 and Figure 8 show two buckling shapes, one with fulfilled and one with unfulfilled minimum stiffness, for a buckling panel under pure longitudinal compression. By complying with the minimum stiffness, local buckling shapes are enforced.

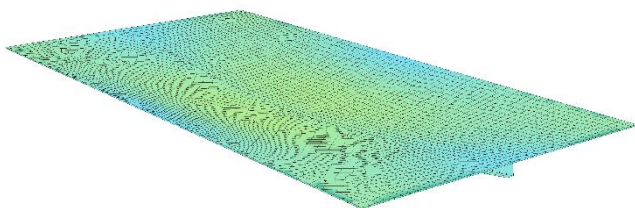


Figure 7 Global buckling mode with unfulfilled minimum stiffness

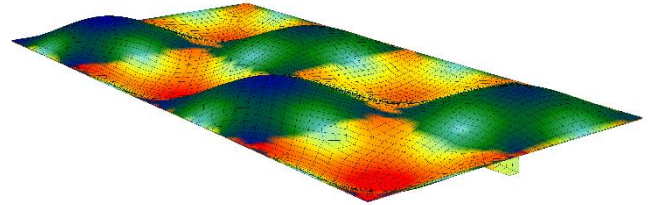


Figure 8 Local buckling mode with fulfilled minimum stiffness

3.3 Panel with a longitudinal stiffener at the third point and a stress state with partial bending $\psi = -0,5$

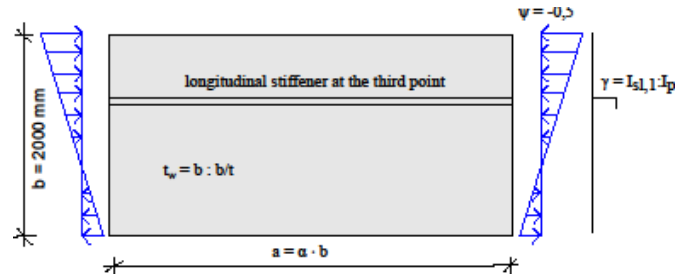


Figure 9 Parameterised buckling field for the investigation of minimum stiffnesses for longitudinal stiffeners at the third point and an edge stress ratio $\psi = -0,5$

In addition to the panel described above with a central stiffener and constant longitudinal compression, the investigation was carried out for a plate with a stiffener at the third point and a stress ratio $\psi = -0,5$. The resulting diagrams for different aspect ratios α are shown below. The results for slender plates largely correspond to the results described above for plates under constant longitudinal compression and central longitudinal stiffener. For stockier cross-sections, the determined minimum stiffnesses are significantly greater compared to the central longitudinal stiffened plates shown above under pure longitudinal compression.

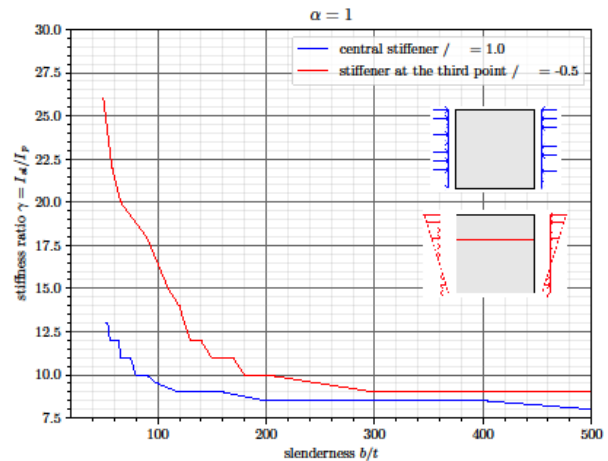


Figure 10 Diagram for minimum stiffness of a longitudinal stiffener for an aspect ratio $\alpha = 1$

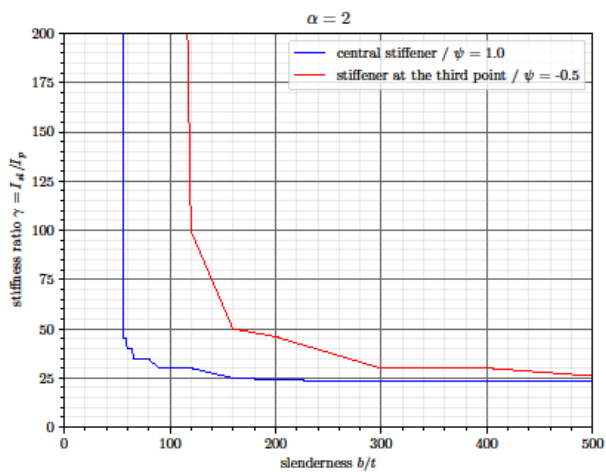


Figure 11 Diagram for minimum stiffness of a longitudinal stiffener for an aspect ratio $\alpha = 2$

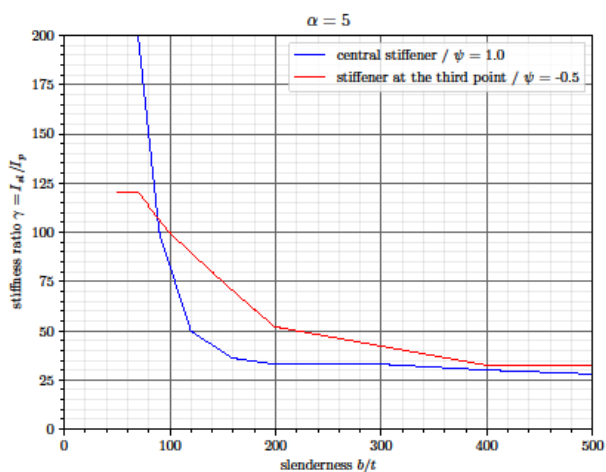


Figure 12 Diagram for minimum stiffness of a longitudinal stiffener for an aspect ratio $\alpha = 5$

3.4 Further investigations on minimum stiffnesses of longitudinal stiffeners

In the course of the master thesis [1], minimum stiffnesses for buckling fields were also investigated under biaxial stress conditions. For biaxial stress conditions (with transverse compression), the required minimum stiffness for long buckling plates increases strongly with increasing deflection due to the additional downward force. As a result, the required stiffness ratios γ also increase strongly. For short buckling plates, on the other hand, the buckling behaviour is still primarily characterised by the longitudinal compression, which is why there is only a small increase in the minimum stiffness. The evaluation in the form of minimum stiffness diagrams has not yet been fully successful due to the complexity.

The buckling of the whole plate including column-like behaviour is not included in the present system. In [1], approaches were investigated to capture the column-like behaviour with the help of buckling verifications on ideal equivalent bars. It was shown that the selected approaches are not suitable for practical use with regard to the accuracy of the results and the applicability.

3.5 Scope and classification of the method

The system presented here for dimensioning plates from diagrams for the buckling verification of the subpanel and a minimum stiffness for a possibly arranged buckling stiffener in relation to the sheet thickness of the base material provides results for the shown "small buckling panels" with a maximum of two longitudinal stiffeners with which the buckling verification of the whole plate is fulfilled in most configurations although this was not explicitly considered. For the general case, especially for large plates with more than two buckling stiffeners, the buckling verification of the whole plate must also be considered in the pre-dimensioning. If in the buckling panel under moment load, the shear component β_τ is more than 10% in relation to the maximum longitudinal compressive stress, an asymmetrical arrangement of buckling stiffeners on the compression side should be dispensed and the longitudinal stiffeners should be arranged evenly distributed over the height. Column-like behaviour of the whole plate in x-direction may have to be investigated separately within the Eurocode.

4 Summary

The developed dimensioning aids for unstiffened plates help, especially in the design phase, to verify buckling with the method of reduced stresses in a target-oriented and fast way. The advantage lies in the very simple and fast determination of results without the evaluation of formulas or using computer programs. In addition, the visual understanding of the interrelationships of the different influencing factors on buckling panels is improved by the graphical representation. In particular, structural engineers who only rarely deal with buckling panel design are supported by a user-friendly and fast verification process in the development of economic solutions. The reduced stress method, which is largely clearly regulated for subpanels, was put into diagrams by converting the formulas. In particular, the dimensioning of stiffener distances or plate thicknesses is very clear. The concept and the developed programme code for creating the diagrams is in principle also suitable for creating further diagrams such as for a one-sided bearing (e.g. flanges with free ends). The diagrams for subpanel buckling presented in this part are used in the context of longitudinal stiffened buckling panels for dimensioning stiffener spacing and plate thicknesses. For the dimensioning of the longitudinal stiffeners themselves, minimum stiffnesses are proposed which were determined with an evaluation of nodal displacements of linearised FEM buckling shapes with the aim of finding a stiffness $I_{sl,1}$ of the longitudinal stiffeners that ensures that subpanel buckling prevails in the buckling shape of the FEM calculation. Diagrams are also created from the data determined in this way which allow sensible pre-dimensioning of longitudinal stiffeners. The developed dimensioning aids help, especially in the design phase, to dimension buckling panels in the mentioned application area in a target-oriented and quick way.

References

- [1] Hulm, F. (2020) *Beitrag zur Entwicklung eines Beulnachweiskonzeptes bei ausgesteiften Beulfeldern auf Basis von Ersatzstabnachweisen* [Master's Thesis]. Technische Universität München.
- [2] DIN EN 1993-1-5:2010-12 *Eurocode 3: Bemessung und Konstruktion von Stahlbauten – Teil 1-5: Plattenförmige Bauteile; Deutsche Fassung EN 1993-1-5:2006 + AC:2009 + A1:2017* (Juli 2017).
- [3] DIN EN 1993-1-5/NA *Nationaler Anhang – National festgelegte Parameter – Eurocode 3: Bemessung und Konstruktion von Stahlbauten – Teil 1-5: Plattenförmige Bauteile* (April 2016)

-
- [4] Python (2020) Python 3.8.6 64-bit [Software]. <https://www.python.org/>
- [5] SOFiSTiK AG (2020) SOFiSTiK 2018-15.0.3 [Software]. <https://www.sofistik.de/>
- [6] Timmers, R.; Schwienbacher, M.; Lener, G. (2019) *Untersuchungen zur Interpretation des Beulnachweises nach der Methode der reduzierten Spannungen*. Stahlbau 88, H. 5, S. 460-469. <https://doi.org/10.1002/stab.201900011>.
- [7] Hertle, R.; Mensinger, M; Ndogmo, J.; Köberlin, T. (2017) *Anmerkungen zum Stabilitätsnachweis längsversteifter Platten unter biaxialem Druck*. Stahlbau 86, H. 2, S. 148-159. <https://doi.org/10.1002/stab.201710461>.
-
1. K³ GmbH, Munich, Germany.
 2. Technical University Munich, Chair of Metal Structures
-